Minimum Atomic Parameter basis sets for elements 1 to 54 in a Hartree-Fock setting

Peter Reinhardt, Ilya Popov, Andrei L Tchougréeff

To cite this version:

Peter Reinhardt, Ilya Popov, Andrei L Tchougréeff. Minimum Atomic Parameter basis sets for elements 1 to 54 in a Hartree-Fock setting. 2021. hal-03135064

HAL Id: hal-03135064
https://hal.sorbonne-universite.fr/hal-03135064v1

Preprint submitted on 8 Feb 2021

Minimum Atomic Parameter basis sets for elements 1 to 54 in a Hartree-Fock setting.

Peter Reinhardt[1], Ilya Popov[2], Andrei L. Tchougréeff[2,3]
[1]*Laboratoire de Chimie Théorique, Sorbonne Université et CNRS UMR7616,*
Paris, France; email: `Peter.Reinhardt@Sorbonne-Universite.fr`
[2]*A.N. Frumkin Institute of Physical Chemistry and Electrochemistry,*
Russian Academy of Sciences, Moscow, Russia
[3]*Institut für Anorganische Chemie, RWTH Aachen, Aachen, Germany*

Abstract

Basis sets featuring single-exponent radial functions for each of the $n\ell$ subshells and orthogonality of the radial parts for different values of n within the same ℓ have been generated for elements 1 to 54 of the Periodic Table, by minimizing the total energy for different spectroscopic states. The derived basis sets can be fairly dubbed as MAP (minimal atomic parameter / Moscow-Aachen-Paris) basis sets. We show that fundamental properties (total energy, radial expectation values, node positions, etc.) of the generated MAP orbital sets are astonishingly close to those obtained with much larger basis sets known in the literature, without numerical inconsistencies. The obtained exponents follow simple relations with respect to the nuclear charge Z. Possible further applications, trends, and limitations are discussed.

Introduction. Why a new set of Slater-like functions to describe atoms?

Quantum chemical modeling starts from finite sets of basis functions so that quality and efficiency of electronic-structure calculations depend on the properties of the latter. This is emphasized in almost every handbook of quantum chemistry (see e.g. Ref. 1) and manifests itself in a wide variety of basis sets used for different objects and their properties.[2–4] Currently, the dominating motivation of quantum-chemical modeling is the accurate numerical reproduction of different properties by using heavy computations. This approach answers questions like "What numerical value has a quantity of interest?" However, a purely numerical approach cannot provide any explanation. A rarely recognized deficiency of this approach is that the experimental data to be numerically reproduced are not available with sufficient accuracy or even definition.[5] An alternative to this numerical approach – which almost disappeared from the literature – aims at a conceptual explanation of experimental trends by using semi-quantitative models. Although this second way sacrifices the numerical accuracy to some extent, these approaches are to be considered as complementary to the former. They, however, need as well basis sets as a starting point, although the requirements differ, as formulated for instance in Ref. 6. In fact, only the following seems to be mandatory for the qualitative or at best semi-quantitative approach: "Each basis function should reflect the nature of the problem, such that a good representation of the orbitals can be achieved by a limited (small) number of functions."[6] If this requirement is satisfied in a consistent way, such that the small number of functions and, thus, of the parameters defining them, is really physically substantiated, then one can hope to be able to fulfill another desideratum, underlined in Ref. 6, namely to provide basis sets for a good fraction of the Periodic Table, and additionally have a regular and sensible dependence of the parameters and basis orbitals on the only true parameter – the atomic number, i.e. the nuclear charge Z.[7,8] This is what we would like to achieve in the present contribution.

The paper is organized as follows. In Section I we provide the theoretical scheme of constructing minimally parameterized sets of atomic orbitals with one single exponent for each $n\ell$ subshell while keeping the correct nodal structure. Next, in Section II, we describe the results of solving the energy-optimization problem for atoms up to $Z = 54$ (Xe) in a restricted-open-shell Hartree-Fock setting, and discuss the obtained results in Section III, in order to draw conclusions (Section IV. A compilation of the data can be found in the accompanying Supplementary Material, and all purely technical details are collected in the Appendix.

I. THEORY

A. The construction procedure

Minimal Slater-based basis sets of the form

$$\varphi_{n\ell m}(\vec{r}) = N_{n\ell}\, P_{n\ell}(2\xi_{n\ell}\, r) e^{-\xi_{n\ell}\, r} \times Y_{\ell m}(\theta,\phi) \tag{1}$$

are defined so that the correct nodal structure of the orbitals (orthogonality between different functions of same ℓ) is maintained by the radial polynomial $P_{n\ell}(2\xi_{n\ell}\, r)$ – the form originally used by Fock and coworkers[9] for the Be atom and for closed $2s^2 2p^6$ shell ions (like Na^+) and then independently rediscovered and employed for the entire 2nd period[10] – leaving the exponents $\xi_{n\ell}$ to be the only free parameters of the basis, as many as subshells. Writing the normalized radial functions as:

$$\begin{aligned} R_{1s}(r) &= N_{1s} e^{-\xi_{1s} r} \\ R_{2s}(r) &= N_{2s}\left(1 + a_{2s}(2\xi_{2s} r)\right) e^{-\xi_{2s} r} \\ R_{3s}(r) &= N_{3s}\left(1 + a_{3s}(2\xi_{3s} r) + b_{3s}(2\xi_{3s} r)^2\right) e^{-\xi_{3s} r} \\ R_{4s}(r) &= N_{4s}\Big(1 + a_{4s}(2\xi_{4s} r) + b_{4s}(2\xi_{4s} r)^2 + \\ &\quad + c_{4s}(2\xi_{4s} r)^3\Big) e^{-\xi_{4s} r} \qquad \ldots \end{aligned} \tag{2}$$

(and similarly for higher values of the angular momentum) and evaluating the general overlap integral

$$\int_0^\infty r^n e^{-\xi_1 r} e^{-\xi_2 r} r^2\, dr = \frac{(n+2)!}{(\xi_1+\xi_2)^{n+3}} \tag{3}$$

we arrive at an iterative scheme as a $2s$ orbital should be orthogonal to $1s$, $3s$ orthogonal to both $2s$ and $1s$ etc, leading together with the normalization to $n-\ell$ conditions for the $n-\ell$ coefficients of the polynomial $P_{n\ell}(2\xi_{n\ell} r)$. The coefficients depend parametrically on the ensemble of ξ's of the functions of lower n. For instance for the $4s$ orbital we obtain 3 equations for the 3 coefficients a_{4s}, b_{4s} and c_{4s}, in a systematic and generalizable manner using reduced exponents $k_{ij} = \frac{\xi_i}{\xi_i+\xi_j}$ with one of the indices i and j being $s4$ and the other running from $1s$ to $3s$.

We can thus determine the orbitals from the exponents $\xi_{n\ell}$ without ambiguity, and optimize the total energy with respect to them. Technically, the total energy for an (open-shell) atom is written, using a non-relativistic Hamiltonian for the atomic system with one or several open shells.[11–13] As no orbital expansion coefficients have to be determined by minimization (they come immediately from the orthonormality condition), one single evaluation of $E_\Psi = \langle\Psi|\hat{H}|\Psi\rangle$ is needed for each set of exponents. The determination of the exponents through the minimization of the total energy is then left to a simplex procedure[14] since the gradients used originally[10] become too cumbersome for the elements beyond the 2nd period. Note that the present procedure is indeed a Hartree-Fock scheme, optimizing the total energy with respect to the parameters of a single-determinant wavefunction, however without the construction and diagonalization of a Fock matrix of the commonly employed Roothaan-Hall procedure.

II. RESULTS

A. Energy minimization and orbital exponents

For the elements $Z = 1 - 54$ (H – Xe) we optimized the exponents for atomic ground states as given by the Aufbau principle, without paying attention to exceptions like Cr, Cu, and most of the $4d$ transition elements. For the same elements we have from the literature the highly optimized multi-exponent Bunge basis sets,[15] which, in terms of total energy, are very close to numerical Hartree-Fock energies.[16] Our basis sets yield total energies slightly higher than the Hartree-Fock limit, about 0.3–0.7 %, which is an amazingly small difference, given the number of free parameters in our calculations. Set aside the proposition of Fock et al.[9], closest to our approach and covering a large part of the periodic table, are the single-zeta basis sets of Clementi and Raimondi,[17] with the same number of exponents as ours, but constructed as optimized linear combinations of nodeless Slater functions. The number of free parameters is thus about twice as large as ours (exponents and expansion coefficients with orthonormality constraints), and the difference to total energies obtained with Bunge's basis sets about a factor two reduced with respect to ours (see Figure 1).

Overlap integrals between core orbitals in the Bunge sets and respective MAP orbitals are found to be larger than 0.99 (> 0.999 for the $1s$ shell), and still larger than 0.90 for

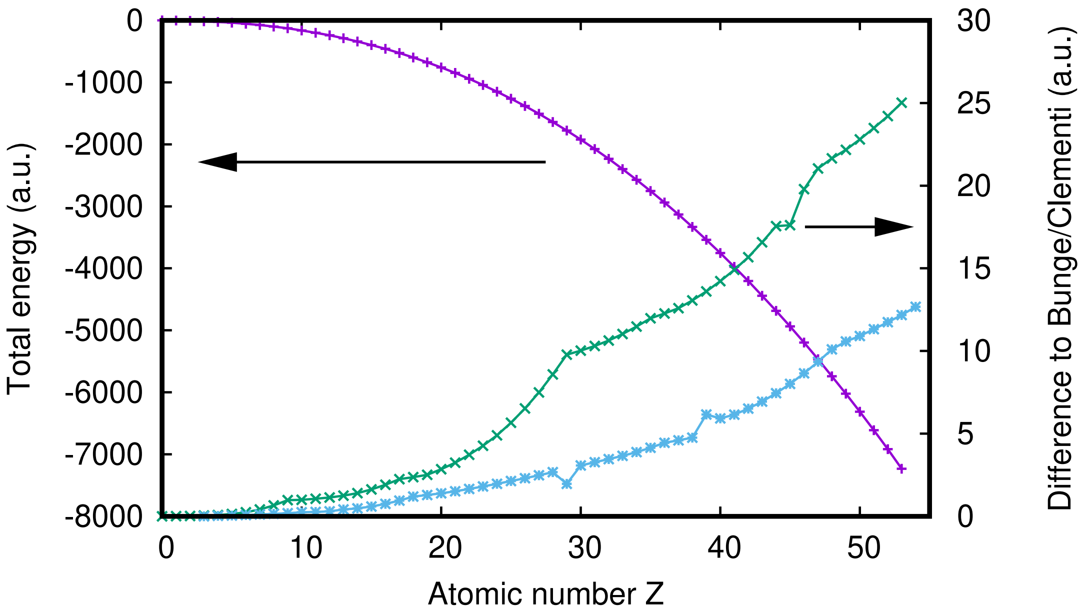

FIG. 1: Total energies (left scale) and difference to Bunge's large basis sets in green and Clementi and Raimondi's[17] single-ζ basis sets in light blue (right scale).

valence orbitals (for more details see below). One exception is the Pd atom for which the basis set of Bunge et al had been determined using the physical $4d^{10}5s^0$ ground state without the need to describe a $5s$ orbital.

Remarkably, in most cases the exponents of valence s-, p- and d-orbitals, determined from the energy minimization procedure, follow, as functions of the atomic number, roughly linear trends as shown in Figure 2, corroborating the semi-empirical argument given in the Introduction.

A closer look reveals that despite almost perfect linear trends particularly for smaller n the deviations from the trends of Figure 2 are not statistical, but systematic. Furthermore, the dependency of orbital exponents with given $(n\ell)$ on the nuclear charge is piecewise linear, clearly visible for instance for the $4s$ exponents in the three groups 19–20 (K and Ca, $4s$ as valence), 21–30 (Sc–Zn, filling of the $3d$ inner shell) and 31–54 ($4s$ being outside of completely filled shells). In Table I we fit the different regions identified for all orbitals to the linear expression $\xi(Z) = a\,Z + b$. The corresponding linear trends are shown in Fig. 3 for $4s$ and $5s$-exponents.

These linear fits, obtained for small Z, may then serve as starting points for the optimization procedure for higher Z, being as reduced as Slater's screening model from 1930,[18]

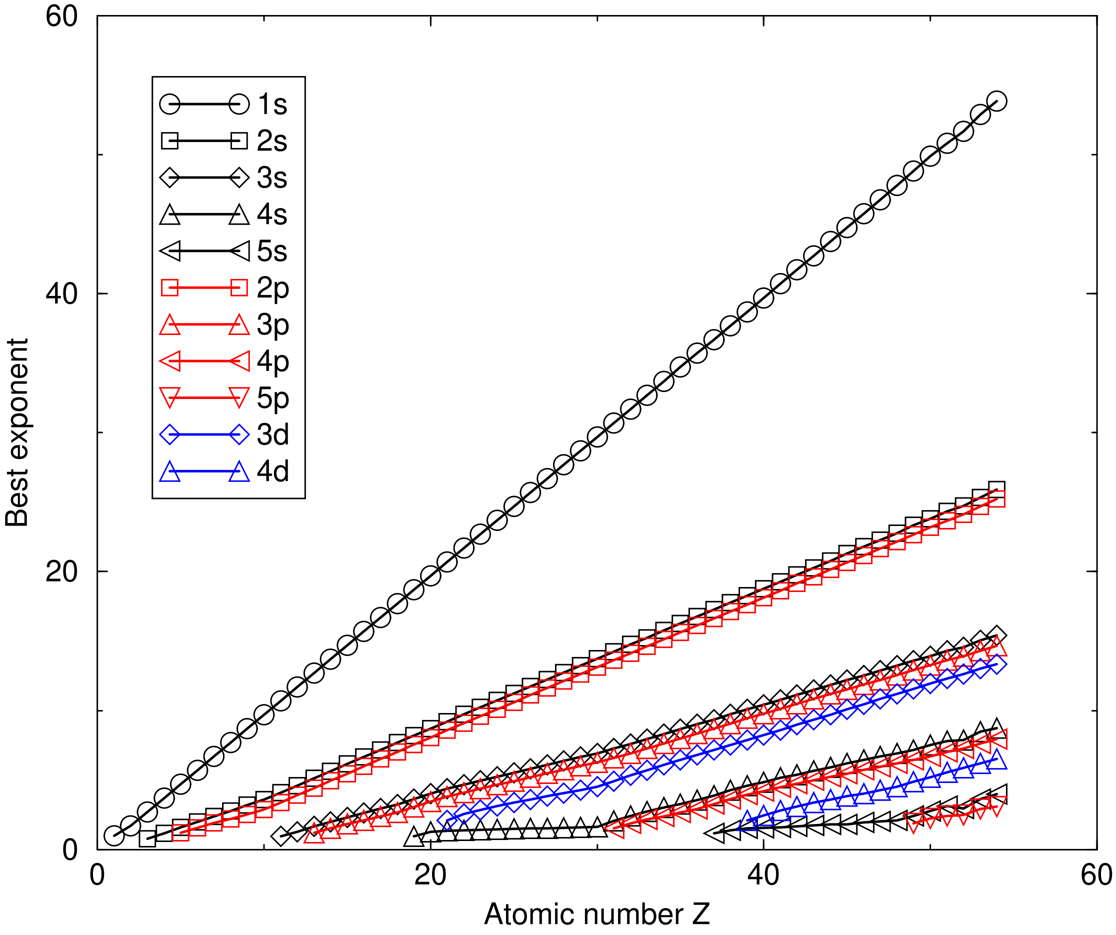

FIG. 2: The optimal exponents as functions of the atomic number Z. The visually almost strait lines coming up to surface up to 3d are in fact misleading: see the text for details.

but including the correct orthogonality of the resulting orbitals through our construction procedure. The ensemble of optimized exponents is collected in the available Supplementary Material. Profiles of the radial parts and corresponding density distributions can be found on a dedicated web site.[19]

B. Position of the nodes of the radial function

Further investigation of the details of the spatial distribution coming from the MAP conjecture, eq. (1), led us to an observation depicted in Figure 4. It can be seen that for a given atom and given value of the azimuthal quantum number ℓ the positions of the nodes of the radial functions $R_{n\ell}(r)$ – the roots of the polynomials $P_{n\ell}(2\xi_{n\ell}\, r)$ – almost coincide

TABLE I: Piecewise linear fits $\xi(Z) = a\,Z + b$ for s, p, and d exponents together with R^2 values. For the 4s and 5s orbitals and the first two elements the character is in quotes as the same orbital is still a valence orbital in the corresponding transition-element series.

Orbital	character	Z-range	a	b	R^2
1s	core	3–54	0.9999	-0.28	1.0000
2s	valence	3–4	0.4017	-0.44	—
2s	core	5–54	0.5046	-1.41	0.9999
2p	valence	5–10	0.3319	-0.45	0.9984
2p	core	11–54	0.5046	-1.41	0.9999
3s	valence	11–12	0.3282	-2.63	—
3s	core	13–54	0.3354	-2.92	0.9985
3p	valence	13–18	0.2878	-2.52	0.9986
3p	core	19–54	0.3326	-3.47	0.9980
4s	“valence“	19–20	0.3135	-5.01	—
3d	valence	21–30	0.2616	-3.23	0.9890
3d	core	31–54	0.3669	-6.42	0.9999
4s	transition	21–30	0.0311	$+0.69$	0.9959
4s	non-transition	31–36	0.3074	-7.53	0.9937
4s	core	37–54	0.2571	-5.50	0.9996
4p	valence	31–36	0.2778	-7.09	0.9947
4p	core	37–54	0.2580	-6.17	0.9996
4d	valence	39–48	0.2756	-8.54	0.9900
5s	”valence“	37–38	0.2812	-9.37	—
5s	transition	39–48	0.0207	$+0.68$	0.9990
5s	non-transition	49–54	0.2686	-11.05	0.9973
5p	valence	49–54	0.2323	-9.47	0.9667

for smaller values of n and for all nodes $k < n - \ell - 1$, counted from the origin, $r = 0$. This is illustrated by the example of the s-orbitals of the Iodine atom, see Figure 5.

This behavior had already been conjectured in the literature[20] in a slightly different context, and, more recently, in a numerical study[21] of the outer spinors in a relativistic

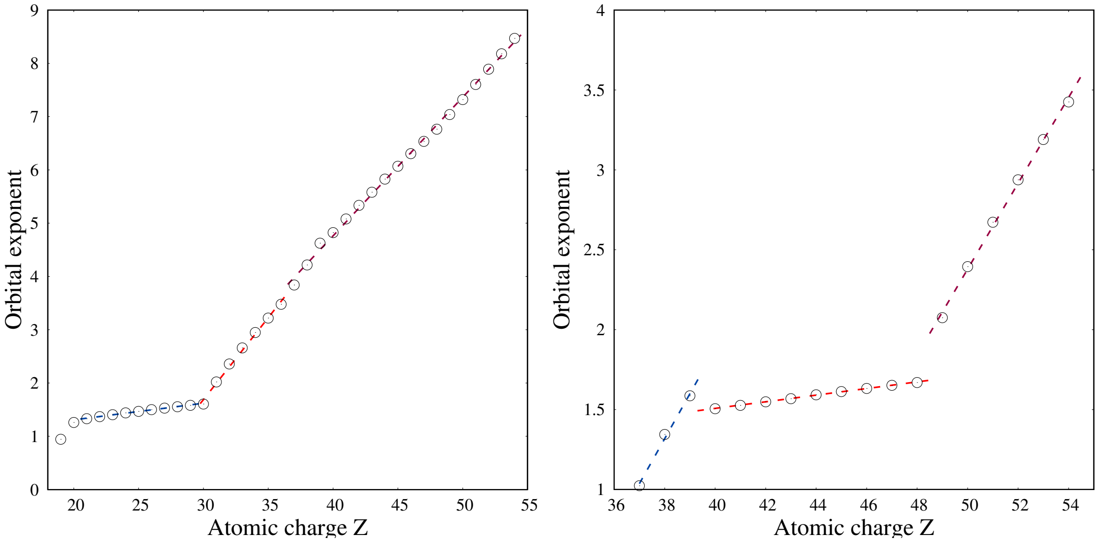

FIG. 3: Piecewise linear trends for 4s (left) and 5s (right) orbital exponents. Yttrium (Z=39) seems an outlier, probably not arrived at the optimum set of exponents. Parameters of all linear fits are assembled in Table I.

setting. It also comes up in the studies on *ab initio* Gaussian atomic basis sets[2,6,22] and may be a general property of all basis-set-expanded atomic orbitals representing, more or less realistic, the atomic one-electron states.

Additionally, we see that the positions of the nodes with the same number, as counted from the nucleus as functions of Z, follow fairly smooth curves, at least for 2s to 4s. They appear in groups, almost coinciding for the respective nodes, starting at the Z values at which further nodes for same ℓ and different n appear.

We observe an evident cusp for the 3rd root of the 4s polynomial between $Z = 30$ and $Z = 31$, at the end of the first transition series. The 4s-exponent is almost constant in this range, but orthogonality has to be achieved with evolving 1s, 2s, and 3s exponents. Beyond $Z = 31$ the 4s exponent varies as well, which adds a different component to the orthogonality constraint, without successive fillings of inner shells. The same is observed for the 5s at $Z = 39$ (Y) and $Z = 48$ (Cd) for the filling of the 4d shell.

III. DISCUSSION

When developing the atomic Hartree-Fock theory in the 1930-1960's (Slater, Roothaan, Clementi) the focus was then on molecular applications, where a purely spherical atom is

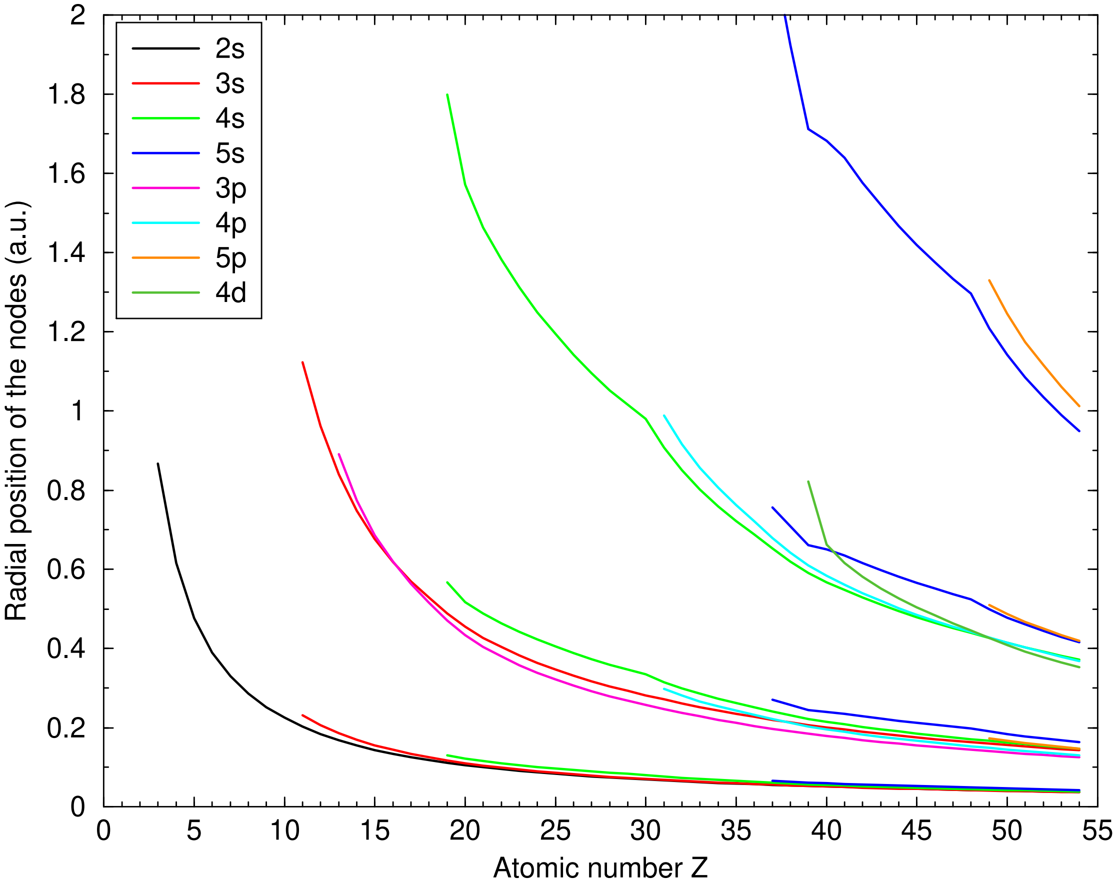

FIG. 4: Position of the nodes of the radial functions $2s$ to $5p$. Multiple lines of the same color refer to the subsequent nodes counted from the origin, $r = 0$, of the same orbital.

an approximation.[23] Our minimally parametrized basis sets are not intended to replace the modern ones designed for molecular applications with numerical precision. They, however, may serve as a set of physical parameters for more qualitative or semi-quantitative studies aimed at establishing and explaining trends in the chemical behavior.

A. Linear trends for the exponents and deviations from them

We may start the analysis of the linear relations described in section II in terms of hydrogen-like orbitals ($\xi = Z/n$) or Slater's parameter set[18]

$$\xi_S^{(n\ell)} = \frac{Z^*}{n^*} = \frac{(Z - \sigma_{n\ell})}{n^*} \qquad , \tag{4}$$

where σ is composed of the screening by the equivalent and inner electrons, and n^* is an effective principal number. As result one obtains as well piecewise linear relations of the

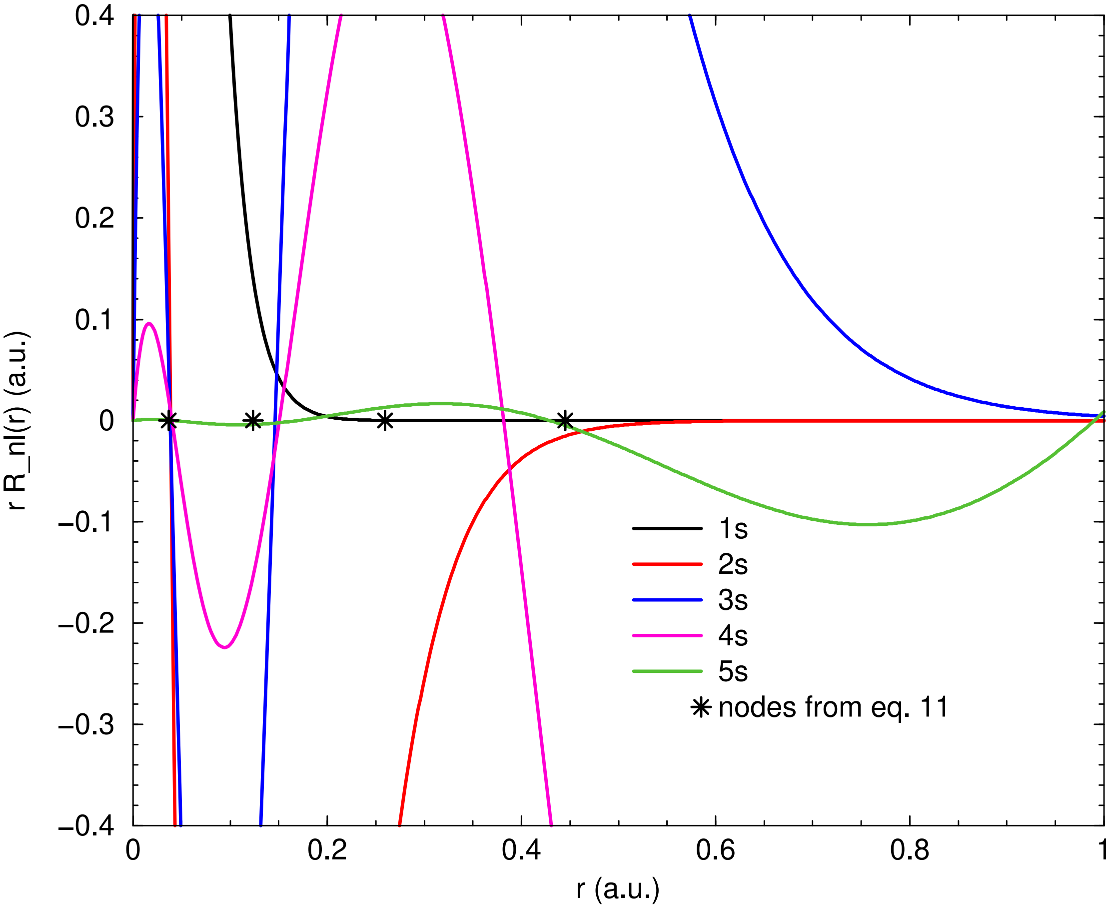

FIG. 5: Plot of the different radial functions of s symmetry for a Iodine atom ($Z = 53$). We clearly see the close coincidence of the first and the second orbital node. Black stars correspond to the estimates described by eq. (11), see Section III C.

effective exponent ξ and the atomic number Z, according to the well-known Slater[18] (or less known Clementi[17]) rules. If an incomplete shell is an outer shell, each step in Z yields an increase of 0.65 in Z^* until the filled shell reaches a maximum screening. Furtheron, each increase in Z adds outer electrons with no influence on the inner shells, thus Z^* increases as Z.

As one can see from Table I, the slopes in the "core" ranges deviate very little from the $1/n$ rule where n is the true principal quantum number – the one determining the number of radial nodes of the function. On the other hand, in the "valence" ranges the slopes for nontransition elements are systematically smaller than $1/n$ – most significantly for $n = 2$, less pronounced for $n = 3$; in either case, however, not precisely following the Slater prescription of $0.65/n$ (which almost exactly shows up for $2p$ valence orbitals only). At $n = 4$ the situation inverts and the slopes of the linear fits of the MAP exponents as functions of Z remarkably exceed $^1/_n$ in the valence range (named non-transition in Table I). This feature is partially absorbed by the effective principal quantum numbers, $n^* < n$, introduced by Slater. However, using n^* instead of n still produces very small slopes in the valence range: the estimate of $0.65/n^*$ based on Slater rules is smaller than the MAP fits in Table I, for which the ratio of slopes between "core" and "valence" trends is more like 1 than 0.65.

The linear relations for valence ns exponents of transition elements show very small slopes (0.03 and 0.02, respectively for $n = 3$ and 4), ultimately meaning that in those series the field felt by s-electrons does not change significantly with the change of the nuclear charge – as expected from Slater's rules ascribing to each electron in the $3d$-shell the screening power of 0.85 relative to the $4s$ electrons. This results in the slopes of $0.15/n^*$ (0.05 and 0.04, respectively) for the latter exponents as functions of Z. This weak increase correlates to the experimental ionization potentials of the $3d$ transition-metal series, spanning a narrow interval of 1.2 eV.

B. Preliminary physics and chemistry implications

As we mentioned in the Introduction, the proposed MAP setting[10] for the atomic orbital basis in its primitive form dating back to 1930-ies[9] has the advantage that its parameters – orbital exponents – have a direct physical significance. Thus, one can hope to relate them more or less directly to some observable characteristics of atoms and eventually those of molecules and crystals/materials. For instance atomic radii may be extracted. Experimentally, these are generally derived by fitting some data on interatomic separations observed in various contexts.

The MAP exponents provide already the size of an atom due to the asymptotically exponential decay of the electron density.[24] A simple measure for an atomic radius is the average radial position $\langle r \rangle$ of the most diffuse orbital. This quantity can be evaluated in any basis set, and we can compare directly orbitals of the Hartree-Fock limit to the MAP orbitals characterized by one single exponent. Figure 6 gives these data for all elements up to Xenon.

The coincidence is again quite striking, atomic radii obtained with the two orbital sets

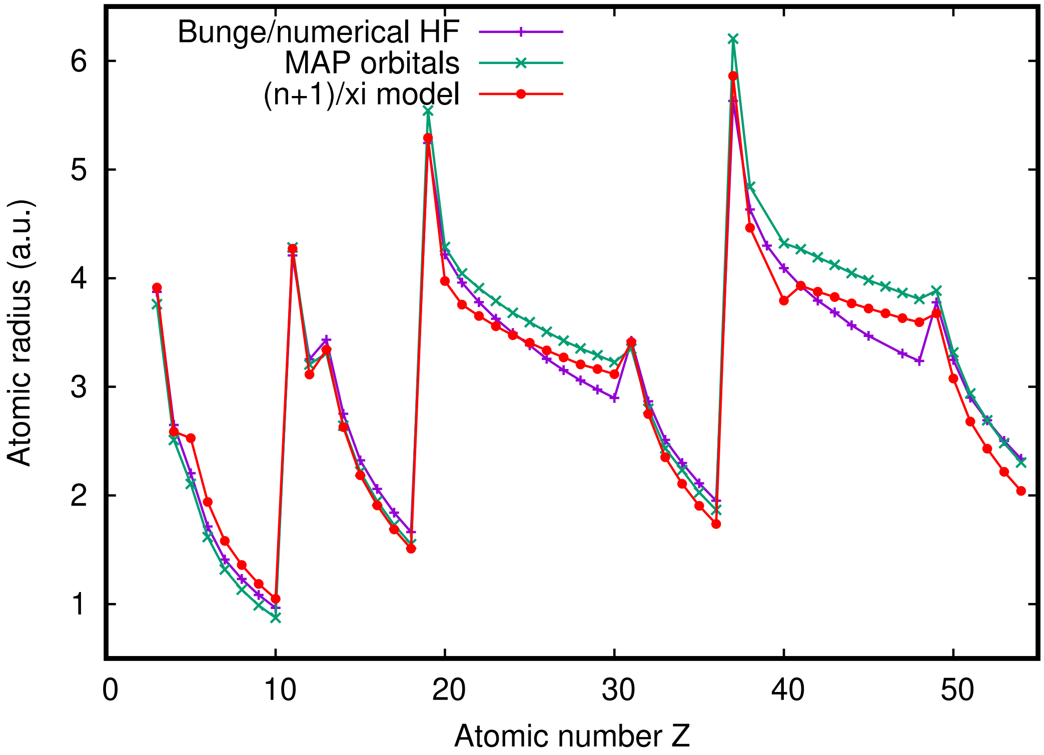

FIG. 6: Atomic radii obtained from Bunge's (violet upright crosses) and the MAP orbitals (green skew crosses), defined as the expectation value $\langle r\rangle$ of the outermost (partially) filled orbital or subshell. For the MAP orbitals we plot as well estimates of the atomic radii as given by eq. 6 (red bullets), see text; the respective interpolating lines are eyeguides.

are nearly superposable, but for the $3d$ and $4d$ transition metals.

Within the MAP philosophy we may develop another way to estimate the atomic size via the the position of the outermost density maximum of its valence shell. For either value of ℓ the highest power of the $P_{n\ell}$ polynomial is $n-1$ so that the dominant contribution to the outermost wave is a simple Slater monomial of the same degree. We can check by fitting a Slater monomial to our MAP orbitals, by maximizing the overlap integral between the two radial functions, dependent on the Slater exponent. We see (Figure 7, upper panel) that the resulting exponents become quite different (about 20%) from the original MAP exponent for the $2s$ orbital of heavier elements, despite r expectation values ($\langle\phi_{\mathrm{Slater}}|r|\phi_{\mathrm{Slater}}\rangle$, $\langle\phi_{\mathrm{MAP}}|r|\phi_{\mathrm{MAP}}\rangle$) being different by only a few pm (Figure 7, lower panel).

Keeping in mind this behavior, we may go back to Figure 5 where we see the quite small oscillations for the $5s$ orbital – the valence MAP states are almost Slater orbitals. For these,

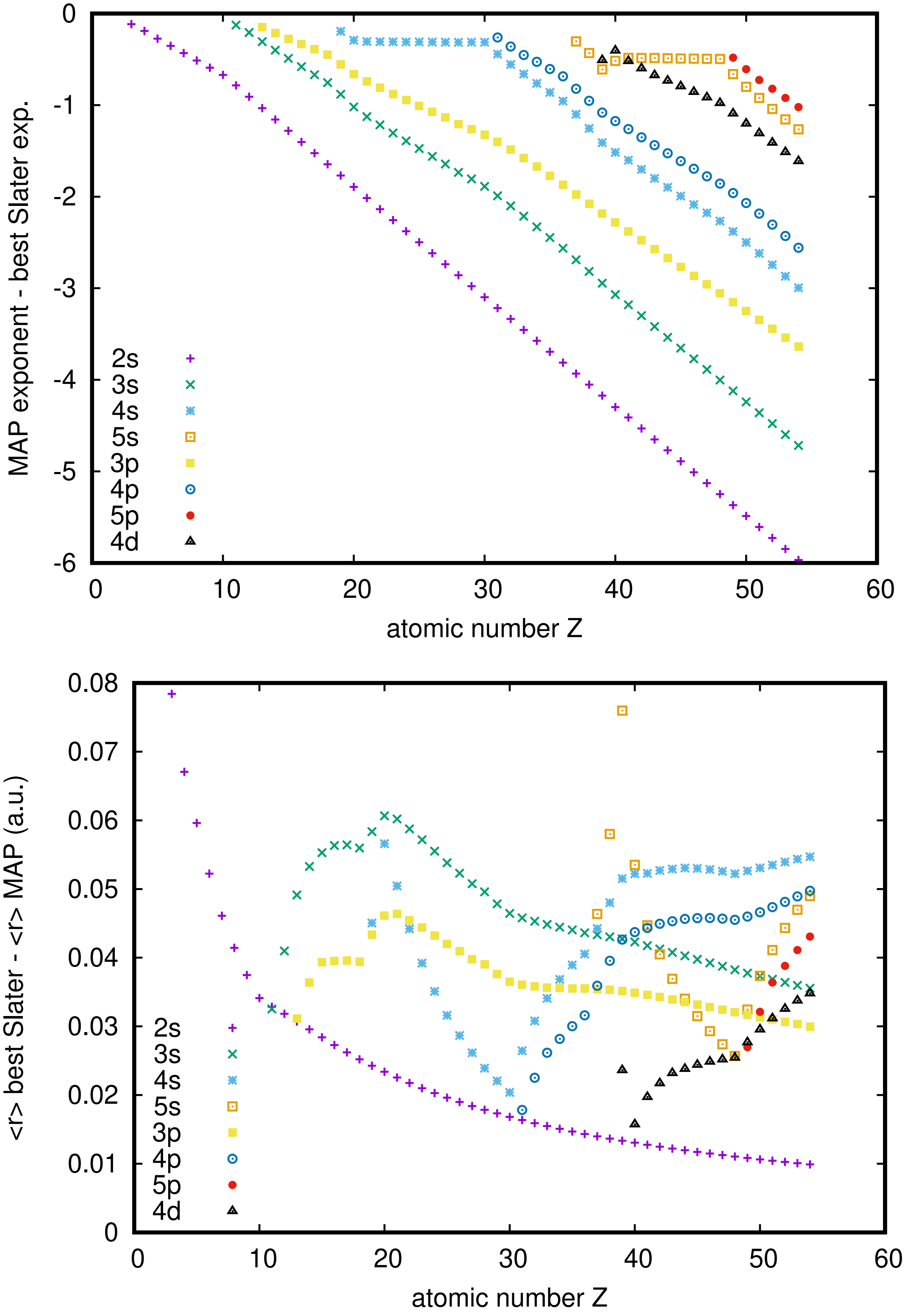

FIG. 7: Difference between MAP exponents and Slater exponents (upper panel), and radial expectation values (lower panel), as function of Z.

the outermost maximum of the radial density $r^2 R_{n\ell}^2\left(r\right)$ is given by the expression

$$r_{\max}\left(Z\right) = \frac{n}{\xi_{n\ell}} = \frac{n^2}{Z - \sigma_{n\ell}\left(Z\right)} \tag{5}$$

where n can be safely understood as the element's period (row) in the Periodic Table.

We add to this value a spherical layer of the thickness of $\xi_{n\ell}^{-1}$ so that ultimately the intrinsic atomic radius reads

$$r_{\mathrm{at}}\left(Z\right) = \frac{n+1}{\xi_{n\ell}} \tag{6}$$

where $n\ell$ refers to the outermost subshell, in particular $4s$ or $5s$ for the transition elements. The resultant data are added to Figure 6. As one can see, this simple estimation generally follows the same trend as the estimates based on $\langle r \rangle$.

C. Nodes of the radial MAP functions

Let us come back to the result of section II B, by looking more in detail at the polynomials $P_{n\ell}(2\xi_{n\ell}\, r)$ which maintain the orthogonality between different functions of the same ℓ.

From the hydrogen atom we have the orthogonality relations involving Laguerre polynomials as

$$\begin{aligned} N_{n\ell} N_{n'\ell} \int_0^\infty & r^{2\ell+2} e^{-2Zr\left(\frac{1}{n}+\frac{1}{n'}\right)} \quad \times \\ \times \quad & L_{n-\ell-1}^{2\ell+1}\left(\frac{2Zr}{n}\right) L_{n'-\ell-1}^{2\ell+1}\left(\frac{2Zr}{n'}\right) dr = \delta_{n,n'} \end{aligned} \tag{7}$$

as the hydrogenic orbital is written as

$$R_{n\ell}(r) = N_{n\ell} r^\ell L_{n-\ell-1}^{2\ell+1}\left(\frac{2Zr}{n}\right) e^{-Zr/n} \qquad . \tag{8}$$

Setting $\xi_{n,\ell} = Z/n$ (or a screened nuclear charge Z_ℓ^*) we arrive at a generalized orthogonality constraint within the MAP series, provided that the exponents for a given angular quantum number ℓ derive from one single Z (or Z_ℓ^*):

$$\begin{aligned} N_{n\ell} N_{n'\ell} \int_0^\infty & r^{2\ell+2} e^{-\left(\xi_{n,\ell}+\xi_{n',\ell}\right) r} \quad \times \\ \times \quad & P_{n,\ell}(2\xi_{n\ell} r) P_{n',\ell}(2\xi_{n'\ell} r)\, dr = \delta_{n,n'} \end{aligned} \tag{9}$$

This is only approximately the case for the Hartree-Fock derived MAP radial parts – we find $\xi_{n,\ell}(Z) \approx {}^{Z}\!/_{n} + b_n$ with a b_n nearly independent of Z, see Table I. The higher Z, the smaller the effect of b_n, which we can formulate as

$$Z \to \infty \ : \quad P_{n\ell}(2\xi_{n\ell}r) \quad \propto \quad L_{n-\ell-1}^{2\ell+1}\left(2\,\frac{Z}{n}r\right) \qquad .$$

However, ignoring the screening (i.e. b_n) comes back to studying a bare, hydrogenoid, atom only, ignoring the poly-electronic situation to describe. Better seems to introduce an average screening for all shells through an effective Z_ℓ^*, averaged over all n, leading to the average setting

$$P_{n\ell}(2\xi_{n\ell}r) \quad \longrightarrow \quad L_{n-\ell-1}^{2\ell+1}\left(2\,\frac{Z_\ell^*}{n}r\right) \qquad .$$

As a consequence, the nodes of the MAP polynomials coincide on average with the corresponding nodes of the associated Laguerre polynomials. The Laguerre polynomials in their turn can be approximated through Bessel functions of the first kind:[25,26]

$$P_{n\ell}(2\xi_{n\ell}r) \propto L_{n-\ell-1}^{2\ell+1}\left(\frac{2Z_\ell^* r}{n}\right) \propto \frac{J_{2\ell+1}\left(2\sqrt{2Z_\ell^* r}\right)}{\sqrt{2Z_\ell^* r}^{\,2\ell+1}} \qquad . \tag{10}$$

From this we can immediately read the position of the roots of the MAP polynomials:

$$r_{n\ell}(k) \approx \frac{j_{2\ell+1,k}^2}{8\,Z_\ell^*} \qquad , \tag{11}$$

where $j_{2\ell+1,k}$ is root number k of the Bessel function $J_{2\ell+1}$ of the first kind, independent of n and inversely proportional to the nuclear charge, corroborating the graphs of Figure 4.

The above estimate basically repeats the old observation based on the WKB treatment of the hydrogen atom (see Ref. 27). For an Iodine atom ($Z = 53$) we have the s exponents ξ_{1s} to ξ_{5s} as 52.6862, 25.2486, 14.8828, 8.1798, and 3.1897, respectively, instead of the hydrogenic Z/n series 53, 26.5, 17.666, 13.25, 10.6. Minimizing the quadratic deviation from the MAP exponents for a common Z_ℓ^* leads to a value of $Z_\ell^* = 49.845$, or an average screening of a little more than 3 electrons.

Via the roots of the Bessel functions $j_{1,k}^2/8$ amounts to 1.8352, 6.1523, 12.9375, 22.1901 and thus expected positions of the nodes are 0.036818, 0.123428, 0.259552, and 0.445178 Bohr from the origin, respectively. We find 0.0431757, 0.168321 0.429621, 0.989825 Bohr as nodes of the 5s orbital which is close for the first node, but more and more off for the subsequent ones. The expected positions are reported in Figure 5.

Of course, the reason for this result is that for the inner shells the screening is fairly correct, and as well the approximation of the Laguerre polynomial via a Bessel function.

For the outer nodes, screening via the chosen Z_ℓ^* becomes quite wrong and the approximation through the Bessel function less reliable.

IV. CONCLUSIONS

Minimally parameterized exponential basis sets of the form eq. (1) originating yet from 1930-ies[9] are defined so that the correct nodal structure (the orthonormality) of the orbitals is maintained through a polynomial depending only on the exponential parameters. Within this setting each (sub)shell can be described by only one single parameter - its orbital exponent. Assuming this we recently explored[10] atoms of the 2nd row of the Periodic Table, and extended the approach up to ($Z = 54$), i.e. including the 5-th period.

The (sub)shell-specific orbital exponents $\xi_{\mathrm{MAP}}^{(n\ell)}$ are derived through optimizing the total energy written in the Hartree-Fock approximation. Overlaps of the obtained orbitals with the corresponding ones from purely numerical approaches or much longer expansions[15] are quite large ($> 90\,\%$) and may serve as basis for atomic projection and subsequent analysis of the results of PAW/DFT calculations.[28] The details of the spatial structure of atomic states, like position of the nodes close to the nucleus or the asymptotic behavior for large r are fairly well reproduced.

Despite the restricted number of free parameters the proposed basis sets result in good total energies, and exponents follow simple piecewise linear relations as functions of the nuclear charge Z. The switches between different linear trends occur either at the end of rows of the Periodic System or when within a row a new (sub)shell starts being filled.

Acknowledgments

This work has been conceived during the stay of P.R. and A.L.T. in Aachen at R. Dronskowski's group whose kind hospitality is gratefully acknowledged. Calculations have been performed mainly in Paris, with the support of the research federation IP2CT to which P.R.

wishes to express his gratitude.

---

[1] *T. Helgaker, P. Jørgensen, J. Olsen*, “Molecular Electronic-Structure Theory”, John Wiley & Sons, New York (2000)

[2] *F. Jensen*, “Atomic orbital basis sets”, WIREs Comput.Mol.Sci. **3** (2012) 273 – 295

[3] *E. Davidson, D. Feller*, “Basis set selection for molecular calculations”, Chem.Rev. **86** (1986) 681 – 696

[4] *V. Blum, R. Gehrke, F. Hanke, P. Havu, V. Havu, X. Ren, K. Reuter, M. Scheffler*, “Ab initio molecular simulations with numeric atom-centered orbitals”, Comp.Phys.Comm. **180** (2009) 2175 – 2196

[5] *B. Civalleri, D. Presti, R. Dovesi, A. Savin*, “On choosing the best density functional approximation”, Sp.Per.Rep., Chem. Mod.: Appl.Theory **9** (2012) 168 – 185 DOI: 10.1039/9781849734790-00168; *P. Pernot, B. Civalleri, D. Presti, A. Savin*, “Prediction uncertainty of density functional approximations for properties of crystals with cubic symmetry”, J.Phys.Chem.A **119** (2015) 5288

[6] *B. Nagy, F. Jensen*, “Basis sets in quantum chemistry”, in Reviews in Computational Chemistry, A.L. Parrill, K.B. Lipkowitz Eds **30** (2017) 93 –149

[7] *A.J. van den Broek*, “Das α-Teilchen und das periodische System der Elemente”, Ann.Phys. **328** (1907) 199–203

[8] *H.G.J. Moseley*, “The High-Frequency Spectra of the Elements. Part II”, Phil.Mag. **6** (1914) 703–713

[9] *V.A. Fock, M.J. Petrashen*, “On the Numerical Solution of Generalized Equations of the Self-consistent Field”, J.Exp.Theor.Phys. **4** (1934) 295 — 325 (engl. version: Phys.Zs.Sowj. **6** (1934) 368)

[10] *I.V. Popov, A.L. Tchougréeff*, “Atomic orbitals revisited: generalized Hydrogen-like basis sets for 2nd row elements”, Theor.Chem.Acc. **138** (2019) 9.

[11] *J.C. Slater*, “Quantum Theory of Atomic Structure, Vol 1”, McGraw Hill, New York (1960)

[12] *C.C.J. Roothaan, P.S. Bagus*, “Atomic Self-Consistent Field Calculations by the Expansion Method”, Methods in Comp.Phys. **2** (1963) 47

[13] *G. Malli*, Technical Report University of Chicago, Dpt Physics, Lab. of Mol. Struc. and

Spectra, 1962/62 Part 2, pages 258-289 available at: `https://digital.library.unt.edu/ark:/67531/metadc228325/m1/`

[14] see for instance *S. Teukolsky, W. Press, W.T. Vetterling*, “Numerical Recipes in FORTRAN77, The art of Scientific computing”, Cambridge University Press, Cambridge (1986) chapter 10.4

[15] *C.F. Bunge, J.A. Barrientos, A.V. Bunge*, “Roothaan-Hartree-Fock Ground-State Atomic Wave-Functions - Slater- Type Orbital Expansions and Expectation Values for Z=2-54”, At.Data Nucl.Data Tables **53** (1993) 113 – 162

[16] *C. Froese-Fischer*, “The Hartree-Fock Method for Atoms: A Numerical Approach”, Wiley Intersciences, New York (1977)

[17] *E. Clementi, D.I. Raimondi*, “Atomic Screening Constants from SCF Functions”, J.Chem.Phys. **38** (1963) 2686 (elements 1-36), and *E. Clementi, D.L. Raimondi, P.W. Reinhardt*, “Atomic Screening Constants from SCF Functions. II. Atoms with 37 to 86 Electrons”, J.Chem.Phys. **47** (1967) 1300

[18] *J.C. Slater*, “Atomic Shielding Constants”, Phys.Rev. **36** (1930) 57

[19] `https://netlab.cartesius.info/ShowPeriodicTable.php`

[20] *M.I. Petrashen, A.B. Ivanova, G. Volf*, “Elementary method of accounting for the influence of the cristalline environment on one-electron s- and p-functions of ions”, Vestnik LGU **10** (1956) 29–38

[21] *A.V. Titov, Y.V. Lomachuk, L.V. Skripnikov*, “Concept of effective states of atoms in compounds to describe properties determined by the densities of valence electrons in atomic cores”, Phys.Rev.A **90** (2014) 052522

[22] *F. Jensen*, “Unifying General and Segmented Contracted Basis Sets. Segmented Polarization Consistent Basis Sets”, J.Chem.Theor.Comput. **10** (2014) 1074

[23] *N. Rosen*, “The Normal State of the Hydrogen Molecule”, Phys.Rev. **38** (1931) 2099

[24] *R. Ahlrichs*, “Asymptotic behaviour of molecular bound state wavefunctions”, Chem.Phys.Lett. **18** (1973) 521

[25] H. Bateman, A. Erdelyi. Higher Transcendental Functions, Vol. 2, 1953, McGraw-Hill Book Company Inc.

[26] G. Szegő. Orthogonal Polynomials. American Mathematical Society, New York City 1959.

[27] *E.U. Condon, G.H. Shortley*, “The Theory of Atomic Spectra”, Cambridge University Press, Cambridge, UK (1959) Chap. 14

[28] *V.L. Deringer, A.L. Tchougréeff, R. Dronskowski*, "Crystal Orbital Hamilton Population (COHP) Analysis as Projected from Plane-Wave Basis Sets", J.Phys.Chem.A **115** (2011) 5461–5466

[29] Original program: *B. Roos, C. Salez, A. Veillard, E. Clementi*, "A general program for calculation of atomic SCF orbitals by the expansion method", IBM Technical Report **RJ 518** (1968) later modified by *L. Donegani, B.A. Heß, and P. Reinhardt*

[30] *F. Jézéquel, J.-M. Chesneaux*, "CADNA: a library for estimating round-off error propagation", Comp.Phys.Comm. **178** (2008) 933–955

Implementation

From a given set of exponents, the linear equations to obtain the coefficients of the polynomials are solved, and a corresponding input for Clementi's atomic Hartree-Fock program[29] is produced. The procedure is easily embedded into a simplex algorithm, as described in standard textbooks of numerical optimization problems.[14] Alternatively to Clementi's program, a local implementation in Moscow (I. Popov) was used,[10] and another specific implementation in Paris of the equations presented in Ref. 12, the latter coupled to the CADNA numerical verification package,[30] for assuring numerical accuracy of the results during the simple optimization procedure, leaving only numerically significant digits in the results. Either of the programs[12,29] runs smoothly for the atoms up to $Z = 54$ (Xe, $5s^2 5p^6$) giving (exactly) the same result as the gradient optimization procedure[10] when it goes about the 2nd period thus confirming the mutual consistency of either protocol.